Acta Biomaterialia 28 (2015) 99–108

Contents lists available at ScienceDirect

Acta Biomaterialia

journal homepage: www.elsevier.com/locate/actabiomat

Designing α-helical peptides with enhanced synergism and selectivity against *Mycobacterium smegmatis*: Discerning the role of hydrophobicity and helicity

Jasmeet Singh Khara [a], Fang Kang Lim [a], Ying Wang [a], Xi-Yu Ke [b], Zhi Xiang Voo [b], Yi Yan Yang [b], Rajamani Lakshminarayanan [c,d], Pui Lai Rachel Ee [a,*]

[a] Department of Pharmacy, National University of Singapore, 18 Science Drive 4, Singapore 117543, Singapore
[b] Institute of Bioengineering and Nanotechnology, 31 Biopolis Way, Singapore 138669, Singapore
[c] Singapore Eye Research Institute, 11 Third Hospital Avenue, Singapore 168751, Singapore
[d] Duke-NUS Medical School, SRP Neuroscience and Behavioral Disorders, Singapore 169857, Singapore

ARTICLE INFO

Article history:
Received 6 April 2015
Received in revised form 31 August 2015
Accepted 14 September 2015
Available online 14 September 2015

Keywords:
Antimicrobial peptides
Amphipathic α-helix
Hydrophobicity
Mycobacterium tuberculosis
Synergy

ABSTRACT

Recently, we reported on a series of short amphipathic α-helical peptides, comprising the backbone sequence $(LLKK)_2$, with the ability to kill susceptible and drug-resistant *Mycobacterium tuberculosis*. In this study, the effect of key physicochemical parameters including hydrophobicity and helicity of α-helical peptides on anti-mycobacterial activity and synergism with rifampicin was investigated. The most hydrophobic analogue, $W(LLKK)_2W$, displayed low selectivity against mycobacteria while peptides with intermediate hydrophobicity were shown to be equally active, yet significantly less toxic. Furthermore, proline substitution impeded the formation of stable amphipathic structures, rendering $P(LLKK)_2P$ as one of the least active analogues. Terminal capping with isoleucine was found to promote α-helical folding and the resultant peptide demonstrated the highest selectivity and minimal cytotoxicity against mammalian macrophages. Flow cytometric analysis revealed that enhancements in hydrophobicity and α-helicity increased the rate and extent of peptide-mediated membrane permeabilization. This finding corroborated the hypothesis that synergism between the peptides and rifampicin was likely mediated via peptide-induced pore formation. The rapid, concentration-dependent membrane depolarization, leakage of intracellular ATP and calcein release from PE/PG LUVs supported the membrane-lytic mechanism of action of the peptides. Together, these findings suggest that hydrophobicity and α-helicity significantly impact anti-mycobacterial activity and optimization of both parameters is necessary to develop synthetic analogues with superior selectivity indices and enhanced synergistic potential with conventional antibiotics.

Statement of significance

There is an urgent clinical need for the discovery of new antimicrobials, effective not just for drug susceptible, but also rapidly emerging drug-resistant TB. Recently, we reported on a series of short amphipathic α-helical peptides, comprising the backbone sequence $(LLKK)_2$, with the ability to kill susceptible and drug-resistant *M. tuberculosis*. In this study, we evaluated a series of synthetic α-helical $(LLKK)_2$ peptides over a range of hydrophobicities for their activity against mycobacteria and provide the first report on the modulating effect of hydrophobicity and α-helicity on the antimicrobial mechanisms of synthetic AMPs and their synergism with first-line antibiotics. These findings demonstrate the applicability of strategies employed here for the rational design of AMPs with the aim of improving cell selectivity and synergistic interactions when co-administered with first-line antibiotics in the fight against drug-resistant tuberculosis.

* Corresponding author.
E-mail address: phaeplr@nus.edu.sg (P.L.R. Ee).

http://dx.doi.org/10.1016/j.actbio.2015.09.015
1742-7061/

1. Introduction

Since the discovery of the first peptide antibiotics, gramicidins, by René Dubos over 70 years ago, scientists have uncovered more than 2000 natural antimicrobial peptides (AMPs) [1]. Though diverse in nature, AMPs possess characteristic features including cationic and amphiphilic regions, both implicated in their ability to kill microbes [2]. Electrostatic interactions between the positively charged peptides, and anionic phospholipids and acidic polymers, drive initial association and accumulation of AMPs onto the bacterial membrane. Upon contacting the lipid bilayer, peptides adopt secondary α or β conformations and either penetrate the hydrophobic membrane core to induce pore formation via barrel-stave or toroidal mechanisms [3,4] or align parallel to the surface and disrupt lipid packing by a "carpet-like" mechanism [5]. Disruption of the bacterial membrane elicits homeostatic imbalances, leakage of intracellular content and eventual cell death [6]. Given their nonspecific membrane-lytic mechanisms, AMPs possess broad-spectrum activities, are rapidly bactericidal and consequently, more resilient to antibiotic resistance development as compared to conventional antimicrobials [7]. These inherent advantages have firmly placed the limelight on AMPs over the past decade as an alternative class of therapeutics to combat the rapid emergence of multidrug-resistant pathogens [8].

Even though mortality and incidence rates have steadily declined since the World Health Organization (WHO) declared tuberculosis (TB) as a global public health emergency over 20 years ago, it still remains the second leading cause of death from an infectious disease today [9]. Multidrug-resistant TB (MDR-TB) remains a prominent threat with an estimated 480,000 new cases in 2013, of which 9.0% contracted extensively drug-resistant TB (XDR-TB), an even more severe form of the disease [9]. The causative agent, *Mycobacterium tuberculosis*, which unlike its Gram-positive counterparts, comprises of a highly complex cell wall and consist of an outer membrane with mycolic acids covalently linked to the peptidoglycan–arabinogalactan polymer [10]. The permeation of hydrophilic solutes across the mycobacterial cell wall mainly occurs through porin channels while lipophilic solutes are able to traverse the lipid-rich outer membrane [11]. As such, it has been suggested that in principle, more lipophilic compounds are expected to exhibit improved activity against mycobacteria due to enhanced intracellular drug uptake [10]. Several research teams have demonstrated that more hydrophobic analogues of fluoroquinolone and isoniazid displayed superior killing properties against *M. tuberculosis* and *M. avium* complex (MAC) [12–14]. Hence, structural modification aimed at enhancing the hydrophobicity of compounds could serve as an effective strategy when designing new antitubercular drugs with enhanced anti-mycobacterial activity.

Interestingly however, majority of the studies employing this strategy on AMPs to date are well focused on Gram-positive and Gram-negative bacteria. Several approaches which have proven effective include the substitution of hydrophobic tryptophan residues, acyl conjugation to the amino terminus, and the inclusion of fluorinated amino acids into peptide sequences [15–17]. To the best of our knowledge, the only study employing this strategy to systematically design and evaluate AMPs for their activity against mycobacteria was met with limited success. In fact, enhancements in peptide hydrophobicity decreased antimicrobial efficacy against *M. tuberculosis*, and this was accompanied by dramatic increments in hemolytic activity of up to 120-fold, resulting in reduced selectivity indices [18]. These findings highlight the long-standing impediment to the clinical application of AMPs: their high systemic toxicity. Hence, the challenge thus far has been to develop compounds with improved microbial selectivity.

Recently, our team demonstrated that peptides designed with the primary backbone sequence $(XXYY)_n$, whereby Y is a cationic amino acid, X is a hydrophobic amino acid, and n is the number of repeat units, adopted ordered helical structures in membrane-like environments [19]. We showed that the antimicrobial peptide $M(LLKK)_2M$ was capable of eradicating both susceptible and drug-resistant *M. tuberculosis* and proposed a membrane-lytic mechanism of action. Keeping in mind the primary objective of developing synthetic analogues with enhanced selectivities, the present study evaluates a series of six synthetic α-helical peptides designed from the parent peptide $(LLKK)_2$ over a range of hydrophobicities for their activity against *M. smegmatis* and eukaryotic cells. The importance of this physicochemical parameter in potentiating the anti-mycobacterial mechanism of action of AMPs against the mycobacterial cell wall, as well as their synergistic activity in combination with rifampicin, was also investigated. Herein, we provide the first report on the modulating effect of hydrophobicity and α-helicity on the antimicrobial mechanisms of synthetic AMPs and their synergism with first-line antibiotics in mycobacteria. Peptide hydrophobicity was experimentally determined using reversed-phase high-performance liquid chromatography (RP-HPLC) and changes in conformation were assessed by circular dichroism (CD) spectroscopy. *In vitro* antimicrobial efficacy was evaluated by MIC and synergy chequerboard assays followed by cytotoxicity studies against rat red blood cell (rRBC) and murine macrophage RAW 264.7 cell line. The anti-mycobacterial mechanisms were investigated by membrane depolarization, flow cytometry and scanning electron microscopy. Membrane destruction triggering the leakage of cytoplasmic content was examined by dye leakage and ATP bioluminescence assays.

2. Materials and methods

2.1. Materials

Dulbecco's modified Eagle's medium (DMEM), dimethylsulfoxide (DMSO, synthesis grade, 99.9%), Tween 80, rifampicin, ethambutol and propidium iodide (PI) were acquired from Sigma–Aldrich (St Louis, MO, USA). Fetal bovine serum (FBS) was obtained from Thermo Scientific Hyclone (Logan, UT, USA). Nutrient broth (Acumedia No. 7146) and bacteriological agar (Acumedia No. 7176) were purchased from Neogen Corporation (Michigan, USA). 3-(4,5-Dimethylthiazol-yl)-diphenyl tetrazolium bromide (MTT) was acquired from Duchefa Biochemie (Haarlem, Netherlands). 3′,3′-dipropylthiadicarbocyanine (diS-C_3-5) dye was purchased from AnaSpec Inc (Fremont, CA, USA). ATP bioluminescence kit was obtained from Molecular Probes Inc (OR, USA). Dry powders of the phospholipids 1,2-dioleoyl-sn-glycero-3-phospho-(1′-rac-glycerol) (DOPG) and 1,2-dioleoyl-sn-glycero-3-phosphoethanolamine (DOPE) were obtained Avanti Polar Lipids, Inc (Alabaster, AL, USA). Phosphate-buffered saline (PBS) solution at 10× concentration was purchased from Vivantis Technologies (Malaysia) and diluted appropriately before use. Rat red blood cells (rRBCs) were obtained from the Animal Handling Units of the Biomedical Research Centers (AHU, BRC, Singapore).

2.2. Mycobacterial and cell culture growth conditions

M. smegmatis (ATCC No. 14468) used in this study was purchased from ATCC (U.S.A.). The bacterial suspension was cultured in nutrient broth containing 0.5% (v/v) Tween 80 and colonies were grown on bacteriological agar. Bacterial stocks were prepared in 15% glycerol and stored at −80 °C. A fresh vial was thawed each time, inoculated into 15 mL of media and incubated at 37 °C and

200 rpm in a shaking incubator for 24 h. Cultures were grown to the mid-log phase with a corresponding optical density reading at 600 nm (OD_{600}) of 0.3, and bacterial density of $\sim 10^8$ CFU mL^{-1}. Mouse macrophage cell line RAW 264.7 was maintained in DMEM supplemented with 10% FBS, 1% penicillin–streptomycin and 44 mM sodium bicarbonate, and cultured in humidified atmosphere at 37 °C and 5% CO_2.

2.3. Peptide characterization

Peptides purchased from GL Biochem (Shanghai, China) were synthesized by standard Fmoc-solid phase methods. Reverse phase (RP)-HPLC carried out by the manufacturer confirmed their purity to be more than 95%. Matrix-assisted laser desorption/ionization time-of-flight mass spectroscopy (MALDI-TOF MS, Model 4800, Applied Biosystems, USA), using α-cyano-4-hydroxycinnamic acid (CHCA) as matrix, was performed to further confirm their molecular weights. An equal volume of peptide solution (0.5 mg mL^{-1} in deionized water) and CHCA solution (saturated in acetonitrile/water mixture at 1:1 volume ratio) was spotted onto the MALDI ground-steel target plate for molecular weight determination.

2.4. Peptide hydrophobicity analysis

The molecular hydrophobicities of the synthetic peptides was analyzed by reverse phase-HPLC on a Shimadzu Prominence UFLC™ system (Shimadzu Corporation, Kyoto, Japan) equipped with a CBM-20A communications bus module, a SPD-20AV UV/Vis detector, a SIL-20A HT autosampler, LC-20AD pumps, a DGU-20A 5 vacuum degasser and a CTO-20A column oven. Runs were performed using an Agilent Poroshell 120 EC-C18 Threaded column (4.6 × 50 mm, particle size 2.7 μm) monitored at 220 nm, with an injection volume of 50 μL and a flow rate of 1 mL min^{-1}. The mobile phase consisted of solvent A (0.1% TFA in water) and solvent B (0.1% TFA in acetonitrile). The gradient profile applied was a 30 min linear gradient from 5% to 50% of solvent B followed by 1 min linear gradient of 5% solvent B and 9 min at 5% solvent B for a total time of 40 min.

2.5. Circular dichroism (CD) spectroscopy

The peptides were first dissolved in 25 mM sodium dodecyl sulfate (SDS) surfactant to a concentration of 0.5 mg mL^{-1}. Peptide solutions were then transferred to a quartz cell with a path length of 1.0 mm and the CD spectra were measured at room temperature with a CD spectropolarimeter (JASCO, J-810). CD spectra were recorded from a wavelength of 190–240 nm, at a scanning speed of 50 nm min^{-1} and averaged from 2 runs per peptide. The acquired spectra were converted to mean residue ellipticity using the following equation:

$$\theta_M = \frac{\theta_{obs}}{10} \cdot \frac{M_{RW}}{c \cdot l}$$

where θ_M is the mean residue ellipticity (deg cm^2 $dmol^{-1}$), θ_{obs} is the observed ellipticity corrected for the blank at a given wavelength (mdeg), M_{RW} is residue molecular weight (M_W/number of amino acids), c is peptide concentration (mg mL^{-1}), and l is the path length (cm).

2.6. Minimum inhibitory concentration (MIC) measurements

The MICs of the antimicrobial agents was determined by the standard broth microdilution method as described previously [19,20]. Peptide stock solutions were prepared in sterile water for all experiments before performing a series of twofold serial dilutions using nutrient broth. Solutions were vortexed for 10–15 s each time to ensure thorough mixing, prior to removing half for dilution. The final drug concentrations ranged from 15.6 to 500 μg mL^{-1} for the peptides, 2–32 μg mL^{-1} for rifampicin and 0.063–2 μg mL^{-1} for ethambutol. 100 μL of the drug solution, together with an equal volume of the bacterial solution at $\sim 10^6$ CFU mL^{-1}, was added to each well of the 96-well plate. The plates were subsequently incubated at 37 °C and 200 rpm in a shaking incubator and read after 72 h. The MIC was defined as the lowest concentration, which inhibits bacterial growth as determined visually, or spectrophotometrically by OD_{600} readings taken by Tecan Infinite 200 Pro (TECAN, Switzerland). Each test was performed in triplicates and repeated three times.

2.7. Chequerboard assay

Antimicrobial interactions between peptides and rifampicin were evaluated via the chequerboard assay as described elsewhere [21,22]. Briefly, 2-fold serial dilutions of rifampicin and each peptide were prepared and added in a 1:1 volume ratio to the wells of a 96-well plate. An equal volume of bacterial solution (100 μL) at $\sim 10^6$ CFU mL^{-1} was then seeded into each well. The plates were incubated in a shaking incubator at 37 °C and 200 rpm and read after 72 h. Bacterial growth was assessed visually or spectrophotometrically via OD_{600} readings taken by Tecan Infinite 200 Pro (TECAN, Switzerland). Each assay was performed in triplicates and repeated three times. The fractional inhibitory concentration index (FICI) for each drug combination was calculated using the following equation:

$$\text{FICI} = \frac{\text{MIC of peptide in combination}}{\text{MIC of peptide alone}} + \frac{\text{MIC of rifampicin in combination}}{\text{MIC of rifampicin alone}}$$

An FICI of $\leqslant 0.5$ was interpreted as synergy, $0.5 < \text{FICI} \leqslant 1.0$ as additive, $1.0 < \text{FICI} \leqslant 4.0$ as indifferent, and an FICI > 4.0 as antagonism [23,24].

2.8. Hemolytic activity test

Freshly drawn rat red blood cells (rRBCs) were diluted 25× with PBS to obtain a 4% (v/v) suspension for subsequent testing. Peptides were serially diluted with PBS to give final concentrations ranging from 0 to 500 μg mL^{-1}. 300 μL of the blood suspension was then mixed with an equal volume of the peptide solution and incubated at 37 °C for 2 h. Following incubation, the mixtures were centrifuged at 1700 g for 5 min and 100 μL of the supernatant was transferred to each well of the 96-well plate. Hemoglobin release was quantified by absorbance measurements at 576 nm by Tecan Infinite 200 Pro (TECAN, Switzerland). Data are expressed as mean ± standard deviation (S.D.) for two independent runs performed in at least four replicates. rRBCs treated with 1% Triton X-100 served as the positive control while untreated rRBCs served as the negative control. The extent of hemolysis was calculated using the following equation:

$$\text{Hemolysis}\ (\%) = \frac{(OD_{576nm}\ \text{of treated sample} - OD_{576nm}\ \text{of negative control})}{(OD_{576nm}\ \text{of positive control} - OD_{576nm}\ \text{of negative control})} \times 100\%$$

2.9. Cytotoxicity testing

MTT assay was performed to determine the cytotoxicity of the peptides against RAW 264.7 cells. The cells were seeded into 96-well plates at a density of 1×10^4 cells per well and incubated overnight at 37 °C and 5% CO_2. Peptides serially diluted in DMEM to give

final concentrations from 3.9 to 250 μg mL^{-1} were then added and the plates further incubated for 24 h. Cells without peptides added served as controls. Following treatment, the media was replaced with 200 μL fresh growth media and 40 μL MTT solution (5 mg mL^{-1}) and incubated for an additional 4 h at 37 °C. Next, 150 μL of DMSO was added to each well to dissolve the resultant formazan crystals and absorbance at 595 nm was measured using Tecan Infinite 200 Pro (TECAN, Switzerland). Cell viability was expressed as $(A_{595nm}$ of treated sample$)/(A_{595nm}$ of control$) \times 100\%$. Data are expressed as mean ± standard error of the mean (S.E.M.) for three independent runs performed in triplicates.

2.10. Flow cytometry

Mycobacterial membrane integrity following peptide treatment was evaluated by flow cytometry. Briefly, *M. smegmatis* suspension was washed twice with PBS and re-suspended at ~10^8 CFU mL^{-1} in the same buffer before treatment with peptides at different concentrations (62.5, 125 and 250 μg mL^{-1}) for 2 h. Peptide stock solutions were prepared in sterile water before performing a series of twofold serial dilutions using nutrient broth. Solutions were vortexed for 10–15 s each time to ensure thorough mixing, prior to removing half for dilution. Next, treated cells were incubated with 20 μg mL^{-1} propidium iodide (PI) for 30 min at 4 °C, followed by washing and re-suspension in PBS to remove any unbound dye. Flow cytometric analysis was performed using CyAn™ ADP Analyzer (Becton Dickinson, San Jose, CA). Each test was reproduced three times and cells treated with rifampicin and ethambutol (1×, 2× and 4× MIC) served as negative controls.

2.11. Field emission scanning electron microscopy (FE-SEM)

M. smegmatis suspension at ~10^8 CFU mL^{-1} was treated with an equal volume of peptide at lethal doses of 250 μg mL^{-1} (4× MIC) or PBS for 2 h. Five replicates were pooled together, centrifuged at 2700 g for 10 min and washed twice with PBS. The samples were then fixed with 4% formaldehyde for 30 min before rinsing with deionized water. A series of ethanol solutions (35%, 50%, 75%, 90%, 95%, 100%) was used to perform sample dehydration, after which they were mounted on copper tapes and allowed to air-dry for 2 days. Samples were finally sputter coated with platinum before imaging under a field emission scanning electron microscope (JEOL JSM-7400F, Japan).

2.12. Cytoplasmic membrane depolarization assay

The ability of the peptides to disrupt mycobacterial membrane potential was assessed using the membrane potential sensitive dye diS-C_3-5. An overnight *M. smegmatis* culture was first washed with 5 mM HEPES buffer containing 20 mM glucose and 0.1 M KCl (pH 7.2) and re-suspended to an OD_{600} of 0.4 in the same buffer. The cells were then incubated with 10 μM of diS-C_3-5 for 1 h at 37 °C after which 600 μL was transferred to a stirred quartz cuvette. Changes in fluorescence intensity following the addition of peptides at 1×, 4× and 8× MIC was monitored using a Quanta Master spectrofluorometer (Photon Technology International, NJ, USA) with an excitation and emission wavelength of 622 and 670 nm respectively.

2.13. ATP bioluminescence assay

Extracellular ATP levels following treatment of *M. smegmatis* with peptides were measured as described previously [25]. Briefly, an overnight *M. smegmatis* culture was first washed and re-suspended in 10 mM phosphate buffer to an OD_{600} of 0.4. Peptides serially diluted with the same buffer to give final concentrations from 15.6 to 500 μg mL^{-1} were then added to an equal volume of bacterial suspension (300 μL) and incubated at 37 °C for 2 h. Next, samples were centrifuged at 5000*g* for 5 min and 50 μL of the supernatant was added to 450 μL of boiling TE buffer (50 mM Tris, 2 mM EDTA, pH 7.8). The mixture was boiled for an additional 2 min and stored on ice until assayed. 100 μL of cooled mixture was added to 100 μL of luciferin-luciferase assay mixture and luminescence was recorded using Tecan Infinite 200 Pro (TECAN, Switzerland). Extracellular ATP concentrations were determined from ATP standard curves using ATP assay kit according to the manufacturer's instructions. Data are expressed as mean ± standard error of the mean (S.E.M.) for three independent runs performed in duplicates.

2.14. Calcein leakage assay

Large unilamellar vesicles (LUVs) loaded with calcein dye were prepared according to methods described previously [26]. Calcein dye was dissolved to a final concentration of 40 mM in 10 mM Na_2HPO_4 in H_2O (pH 7.0). 476 μL PE and 127 μL PG dissolved in 25 mg mL^{-1} $CHCl_3$ were mixed in a round bottom flask. Solvent removal by rotatory evaporator left behind a thin lipid film, which was then hydrated using 1 mL calcein solution. The mixture was stirred for an additional hour on the rotary evaporator at atmospheric pressure before being subjected to ten freeze–thaw cycles (dry ice/acetone to freeze and warm water to thaw). Extrusion of the suspension was then carried out twenty times through a polycarbonate membrane with 400 nm pore diameter. Removal of excess dye was performed using a Sephadex G-50 column, with a buffer consisting of 10 mM Na_2HPO_4 and 90 mM NaCl as the eluent. Dye-filled LUVs were then diluted 2000 times using the same buffer to achieve a final lipid concentration of approximately 5.0 mM. The calcein fluorescence emission intensity I_t (λ_{em} = 515 nm, λ_{ex} = 490 nm) was measured following treatment of LUVs with peptides at various concentrations (125, 250 and 500 μg mL^{-1}) for 1 and 2 h. Fluorescence emission following addition of 50 μL Triton X-100 (20% in DMSO) (I_x) was taken as 100% leakage while the baseline (I_0) was measured without peptide addition. Treatment with pure DMSO did not produce any leakage. The percentage of calcein leakage was calculated as follows:

$$\text{Leakage } (\%) = (I_t - I_0)/(I_x - I_0) \times 100\%$$

2.15. Killing efficiency test

M. smegmatis was treated with antimicrobial peptides at concentration corresponding to 0.5×, 1×, 2×, 4× and 8× MIC. 100 μL of bacterial solution at ~10^6 CFU mL^{-1} was seeded into each well of a 96-well plate and an equal volume of peptide solution was added. Following incubation at 37 °C for 72 h, samples were serially diluted in nutrient broth for determination of viable counts. 10 μL of the diluted samples were plated in triplicates onto agar plates and incubated at 37 °C for another 72 h before total bacterial counts were measured. The results are expressed as mean log (CFU mL^{-1}) ± standard deviation. The antimicrobial peptide I $(LLKK)_2I$ was evaluated in this study as it displayed the highest selectivity towards microbial over mammalian cells.

3. Results and discussion

3.1. Peptide design and characterization

The interactions between peptides and bacterial membranes are modulated by various physicochemical properties including

peptide hydrophobicity, charge, secondary structure, and amphiphilicity [27,28]. In order to elucidate the influence of hydrophobicity on their antimicrobial activity, synthetic peptides were designed with minimal sequence modification to maintain their charges and amphiphilicity fairly unaltered. To achieve this, $(LLKK)_2$ was used as a framework to systematically modify peptide hydrophobicity by substituting amino acids to both the N- and C-terminals to obtain peptides with the backbone sequence X$(LLKK)_2$X, where X is a hydrophobic amino acid. Five amino acids, methionine, cysteine, proline, isoleucine and tryptophan were selected to obtain the following peptides: M$(LLKK)_2$M, C$(LLKK)_2$C, P$(LLKK)_2$P, I$(LLKK)_2$I and W$(LLKK)_2$W, which will henceforth be referred to as per their abbreviated denotations listed in Table 1. The C-terminal of all six analogues was amidated to improve antimicrobial activity by conferring peptides with an extra net positive charge [29,30]. The fidelity of peptide synthesis was confirmed via MALDI-TOF MS and the results are summarized in Table 1. The close agreement between the measured and theoretical molecular weights of the peptides indicates that the compounds were synthesized to the desired specifications. The overall hydrophobicity of the peptides was measured by their retention time (t_R) using RP-HPLC and ranged from 15.68 to 24.40 min as shown in Table 1. The parent peptide LK without any additional amino acid residues recorded the lowest t_R of 15.68 min while WW, with two extra tryptophan residues, displayed the greatest hydrophobicity with a corresponding t_R of 24.40 min. The ranking of the peptides in terms of increasing overall hydrophobicity is as follows: LK < PP < CC < II < MM < WW.

3.2. Circular dichroism spectroscopic studies

The secondary structure of the synthetic peptides in a membrane-like environment was studied using CD spectroscopy and the results are summarized in Fig. 1. The peptides adopted α-helical structures in 25 mM SDS solution as confirmed by the presence of the double minima at ~208 and 222 nm. Generally, the addition of amino acids to both the N- and C-terminals resulted in greater α-helical conformation as determined by a more negative mean residue ellipticity value at 222 nm (θ_{222}). Although, the value at θ_{222} is commonly used to determine the degree of helicity of peptides, these estimates tend to be less accurate for short helices [31]. Hence, the percentage α-helicity of synthetic peptides was calculated using an equation described by Baldwin and subsequently modified by Fairlie, given by the ratio of $\theta_{222}/\theta_{max}$, and θ_{max} is calculated using the following equation:

$\theta_{max} = (-44000 + 250T)(1 - \frac{k}{n})$, where T is the temperature in °C, k is the finite length correction and n is the number of peptide residues [32,33]. The θ_{max} for 8 and 10 residue helices is −19,500 and −23,400 respectively when k = 4 and T = 20 °C. The percentage helicity of the peptides is summarized in Table 1. Of the six, LK and

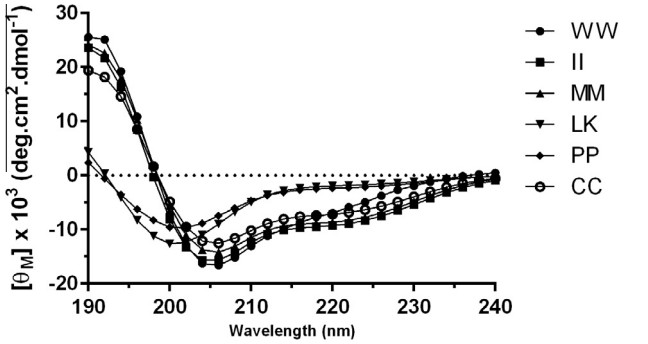

Fig. 1. CD spectra of synthetic peptide analogues displaying characteristic double minima at ~208 and 222 nm, confirming their α-helical secondary conformations.

PP were found to possess the lowest α-helical contents of about 9%, while the α-helicity of the other four peptides was three to four folds greater. These findings suggest that increasing peptide hydrophobicity results in an increase in α-helical structure, consistent with reports by other research groups, which found that increasing hydrophobicity correlated with increasing α-helical content [34,35]. Only PP did not conform to this trend as its enhanced hydrophobicity as compared to LK did not improve its propensity for α-helical folding. This finding implies that factors other than hydrophobicity may be modulating the helical propensity of the proline substituted analogue. One possibility could be that steric hindrance induced by the bulky pyrrolidine ring present in proline residues, gives rise to conformational distortion in the preceding helical turn, thus hindering the formation of stable α-helices [36,37]. A more likely reason however, is that the inclusion of proline in the middle of helices or near the C-terminal can cause breakage of adjacent hydrogen bonds and premature termination of the helix [38,39]. This could have in turn mitigated the effects of increasing hydrophobicity on α-helicity, resulting in similar α-helical contents as seen for both LK and PP.

3.3. In vitro anti-mycobacterial activity

The antimicrobial activities of the synthetic peptides and rifampicin against *M. smegmatis* determined by the broth microdilution method are summarized in Table 2. The peptide analogues displayed varying efficacy against *M. smegmatis* with MICs ranging from 62.5 to 250 μg mL^{-1}. Overall, hydrophobic modifications to LK produced three analogues with improved antimicrobial activity while the other two inhibited bacterial growth less effectively. The addition of tryptophan, methionine and isoleucine residues to both the N- and C-terminals enhanced the potency of LK, reflected by the decrease in MIC from 125 to 62.5 μg mL^{-1} for WW, MM and II. While enhancing the hydrophobicity of α-helical peptides has been shown to improve antimicrobial activity, high peptide

Table 1
Amino acid sequence of synthetic cationic α-helical peptide analogues and their physiochemical parameters including charge, hydrophobic moment, hydrophobicity and helicity.

Amino acid sequence	Peptide denotation	Theoretical M_w	Measured M_w[a]	Net charge	μH[b]	t_R[c] (min)	% helicity[d]
LLKKLLKK-NH_2	LK	982.37	983.02	+5	3.69	15.68	9.3
PLLKKLLKKP-NH_2	PP	1176.60	1177.02	+5	3.69	17.80	9.7
CLLKKLLKKC-NH_2	CC	1188.66	1187.51[e]	+5	3.69	20.76	29.3
ILLKKLLKKI-NH_2	II	1208.69	1209.14	+5	3.69	21.63	38.1
MLLKKLLKKM-NH_2	MM	1244.76	1245.18	+5	3.69	21.69	35.4
WLLKKLLKKW-NH_2	WW	1354.79	1355.15	+5	3.69	24.40	25.1

[a] Measured by MALDI-TOF MS, apparent $M_w = [M_w+H]^+$.
[b] The hydrophobic moment (μH) was determined by the totalizer module of Membrane Protein Explorer (MPEx) which uses the experimentally based interfacial Wimley–White hydrophobicity scales and is available online at http://blanco.biomol.uci.edu/mpex.
[c] Retention time as determined by RP-HPLC.
[d] % helicity was calculated from ratio of $[\theta]_{222}/[\theta]_{max}$ using a modified Baldwin equation as described in Section 3.2.
[e] An additional dimer peak was observed at m/z 2374.78 for CC.

Table 2
Minimum inhibitory concentrations (MICs), fractional inhibitory concentration indices (FICIs), and selectivity indices (SIs) of synthetic antimicrobial peptides against *M. smegmatis*.

Antimicrobial agent	MIC (μg mL^{-1})		FIC	FICI[a]	HC_{50} (μg mL^{-1})	SI[b]
	Alone	Combination				
$(LLKK)_2$	125	62.5	0.5	0.75 (A)	>500	8
$P(LLKK)_2P$	250	125	0.5	0.75 (A)	>500	4
$C(LLKK)_2C$	250	250	1.0	1.25 (I)	>500	4
$I(LLKK)_2I$	62.5	15.6	0.25	0.50 (S)	>500	16
$M(LLKK)_2M$	62.5	15.6	0.25	0.50 (S)	>500	16
$W(LLKK)_2W$	62.5	15.6	0.25	0.50 (S)	363	5.8

[a] Antimicrobial interactions were classified as additive (A), indifferent (I) or synergistic (S).
[b] Selectivity index (SI) is determined as follows: (HC_{50}/MIC). When no detectable hemolysis was observed at the highest tested concentration of 500 μg mL^{-1}, a value of 1000 μg mL^{-1} was used for TI calculations.

hydrophobicity is associated with stronger peptide self-association resulting in the formation of dimers/oligomers [34,40]. This in turn correlates with weaker antimicrobial activity since peptide dimers/oligomers are prevented from readily passing through the bacterial capsule and cell wall in order to reach their target plasma membrane. This could explain why the most hydrophobic peptide, WW, did not show a corresponding improvement in its MIC against *M. smegmatis* as compared to less hydrophobic analogues, MM and II. Surprisingly, despite its increased hydrophobicity and α-helicity, CC demonstrated poorer anti-mycobacterial activity as compared to LK. Since CC is less hydrophobic than MM, II and WW, any peptide self-association resulting in dimer/oligomer formation should not significantly compromise its activity as compared to the three most hydrophobic analogues. Yet it was found to be the least potent analogue, which implies that another factor unique to this peptide alone might be responsible for this observation. Further discussions on the diminished activity of CC will be carried out in Section 3.6, together with the flow cytometric analysis. As for PP, it is likely that the reduced propensity for helical formation observed (Fig. 1) was responsible for the decrease in antimicrobial potency as compared to WW, MM and II. A decrease in α-helicity by the introduction of proline residues into helices has been shown to greatly reduce the antimicrobial efficacy and activity spectrum of α-helical peptides [41]. This finding suggests that peptide helicity is another important parameter which should be given due consideration when looking to design more potent peptides. Even though our findings highlight that flanking of both the N- and C-terminals with proline can produce detrimental effects on antimicrobial potency, the incorporation of proline residues in peptides should not be dismissed entirely as an ineffective strategy in designing more selective analogues. A recent study found that the careful substitution of proline residues into peptide sequences can in fact reduce cytotoxicity and improve antibacterial selectivity [42].

3.4. Hemolytic activities and cell selectivities

The hemolytic activities of the synthetic peptides were evaluated using 4% (v/v) rat blood as a measure of their toxicity against mammalian cells, and the results are summarized in Fig. A2A found in the supplementary data. The HC_{50} values, defined as the peptide concentration producing 50% hemolysis of rRBCs, are shown in Table 2. Except for WW, all the other five peptides exhibited very low hemolysis (⩽3%) even up to concentrations of 500 μg mL^{-1}. Notably, all six peptide analogues induced minimal hemolysis (⩽3%) at their respective MICs. The most hydrophobic peptide, WW, displayed the strongest hemolytic activity of ~19% and 69% at 250 and 500 μg mL^{-1} respectively. This corresponded to a far lower HC_{50} value of 363 μg mL^{-1} for WW as compared to the other peptides (>500 μg mL^{-1}). While the modulating effect of hydrophobicity on the hemolytic activity of the peptides was evident, the contribution of α-helicity was far less apparent. The two most helical peptides, MM and II, were minimally hemolytic even at 500 μg mL^{-1}, suggesting that hydrophobicity, rather than helicity, was more likely the driving force behind the enhanced hemolytic activity observed for WW. Previous studies examining the membrane permeabilization of electrically neutral POPC vesicles by peptide analogues of varying hydrophobicity have also shown that increasing hydrophobicity produced a greater degree of hemolysis [43,44]. This phenomenon was attributed to the zwitterionic nature of eukaryotic membranes, which facilitates deeper penetration of more hydrophobic peptides thus inducing greater pore formation and consequently, stronger hemolysis.

The selectivity indices (SIs) shown in Table 2, defined as the ratio of HC_{50} to MIC values, serve as a measure of antibacterial selectivity, with larger SI values indicative of greater selectivity towards microbial over mammalian membranes. MM and II proved to be the best analogues (SI = 16), while the most hydrophobic analogue, WW, had a lower selectivity index as compared to LK. Previous studies have also shown that increasing peptide hydrophobicity may decrease antimicrobial selectivity of α-helical peptides [18,45]. However, the findings presented in this study suggest that moderate increase in peptide hydrophobicity can translate into better selectivity, as seen for MM and II, but further increments could produce deleterious effects on peptide selectivity, as observed for WW.

3.5. Cytotoxic effect of peptides on macrophages

The cytotoxicity of the peptides against mammalian cells was further evaluated against RAW 264.7 macrophage cell line and the results are shown in Fig. A2B found in the supplementary data. LK, PP and II were found to be the least cytotoxic analogues with cell viabilities in excess of 85% even up to concentrations of 250 μg mL^{-1}. The most hydrophobic analogue, WW, was also the most cytotoxic, recording the greatest reduction in cell viability from 92.3% to 13.2% with an increase in concentration from 3.95 to 250 μg mL^{-1}. At MIC concentrations (62.5 μg mL^{-1}), approximately 50% of the cells treated with WW remained viable, whereas for MM and II, which also had similar MICs, cell viabilities were higher at 77.9% and 98.5% respectively. Similar to the trends observed with regards to their hemolytic activities, hydrophobicity was found to be a more significant contributor towards cytotoxicity than the α-helical character of the peptides. This observation is in line with previous findings reported by Jacob and coworkers who also found that increasing the hydrophobicity of α-helical peptides induced greater cytotoxicity against RAW 264.7 cells [46]. Interestingly, despite its superior hydrophobicity and helicity, the isoleucine substituted analogue II possessed a comparable cytotoxicity profile to LK even up to 250 μg mL^{-1}. Though the hydrophobic and helical characters of MM and CC were comparable to II, both were found to be more toxic towards mammalian cells with 80% cell viabilities even at 15.6 μg mL^{-1} (Fig. A2). Given that macrophages are potentially major reservoirs for mycobacteria during pulmonary TB infection, the incorporation of isoleucine as compared to other hydrophobic amino acids such as methionine, cysteine and tryptophan, may be a more suitable when designing potent peptides with reduced cytotoxicity against mammalian cells.

3.6. Flow cytometry

To investigate the extent of membrane disruption induced by the peptide analogues, *M. smegmatis* was treated with all six peptides in the presence of the DNA intercalating agent propidium iodide (PI). Peptide-mediated destruction of the bacterial membrane is expected to facilitate the intracellular diffusion of PI and the proportion of bacterial cells fluorescently stained by PI following incubation with peptides at various concentrations (62.5, 125 and 250 μg mL^{-1}) is summarized in Fig. 2. First-line antitubercular agents, rifampicin and ethambutol, served as negative controls given that they target DNA-dependent RNA polymerases and arabinosyl transferases respectively, rather than the mycobacterial membrane directly. Both drugs resulted in staining of approximately 1% of bacterial cells at 1×, 2× and 4× MIC implying that mycobacterial membrane integrity remained largely uncompromised (Fig. A3A found in the supplementary data). Interestingly, >99% of cells treated with LK and PP did not present any fluorescent signal even up to concentrations of 250 μg mL^{-1}, indicative of intact bacterial cell membranes. This implies that the anti-mycobacterial mechanism of action of both these peptides could be different from that of the other peptides. In contrast, treatment with the three most hydrophobic peptides, WW, MM and II resulted in a significant concentration dependent increase in proportion of bacterial cells taking up the fluorescence dye. At concentrations equivalent to MIC, 63.8%, 88.3% and 84.0% of cells were stained with PI following treatment with WW, MM and II respectively. The stronger membrane-permeabilizing capacity of these peptide analogues could be attributed to their higher hydrophobic and α-helical character as compared to LK and PP. Notably, we found that helicity was more closely correlated to PI uptake as compared to hydrophobicity (Fig. A3B found in the supplementary data). This suggests that the folding of the synthetic peptides into amphipathic structures was necessary for the penetration of peptides into the hydrophobic core and subsequent disruption of the lipid bilayer in bacterial cell membranes. As for CC, only 6% of cells were stained with PI even up to concentrations of 250 μg/ml. A plausible explanation for this observation could be the dimerization/oligomerization of CC monomers, driven not by self-association, but by the oxidation of reactive sulfhydryl groups present in cysteine residues. MALDI-TOF MS analysis covering up to 10,000 Da confirmed the formation of dimers as a distinct peak was observed at *m*/*z* 2374.78 (Fig. A1 found in supplementary data). However no oligomer formation was observed. It is likely that these CC dimers are prevented from readily penetrating the mycobacterial cell wall to reach the target cytoplasmic membrane, thus reducing its antimicrobial efficacy.

3.7. Synergistic antimicrobial interactions

Given that combinatorial drug regimens is the cornerstone of successful anti-TB chemotherapy, the potential for synergistic interactions between the peptides and rifampicin was assessed by the chequerboard assay. As shown in Table 2, none of the six synthetic peptides demonstrated antagonistic activity when treated in combination with rifampicin. The three most effective peptides WW, MM and II exhibited synergism with a FICI of 0.5 against *M. smegmatis* while LK and PP both displayed an additive effect with rifampicin (FICI of 0.75). The combination of CC and rifampicin was interpreted as indifferent with a FICI value greater than 1. The mechanism behind this observed synergism could be attributed to the membrane-permeabilizing activity of peptides that compromises membrane integrity. This in turn allows for the increased uptake of rifampicin into the cells and enhances its accessibility to intracellular targets [47,48]. As such, peptides with superior membrane-disrupting properties would be expected to better facilitate the cytoplasmic entry of rifampicin and consequently demonstrate stronger synergistic interactions. The flow cytometric analysis revealed that LK and PP possessed poor membrane-permeabilizing activity (Fig. 2), which lends support as to why they were additive with rifampicin while WW, MM and II, synergistic. Due to their lower hydrophobic and α-helical propensity, LK and PP possessed weaker membrane disrupting properties and hence, a higher concentration of these two peptides was required to inhibit bacterial growth as compared to WW, MM and II (62.5 and 125 versus 15.6 μg mL^{-1}) when co-administered with the same amount rifampicin (0.98 μg mL^{-1}).

3.8. Antimicrobial mechanisms of action

The ability of peptides to perturb the phospholipid bilayer was investigated by determining the dye leakage from calcein-loaded LUVs composed of PE/PG lipids (4:1). As shown in Fig. 3, II induced calcein release from the bacterial membrane-mimicking vesicles in a concentration- and time-dependent manner. As compared to LK, ⩾4-fold increment in dye leakage was observed for II at all concentrations tested. The more hydrophobic and helical nature of II, in comparison to LK, is likely responsible for its stronger membrane-permeabilizing properties. This in turn translated into improved anti-mycobacterial efficiency, evident from the lower MIC and FICI values seen for II (Table 2). These results are

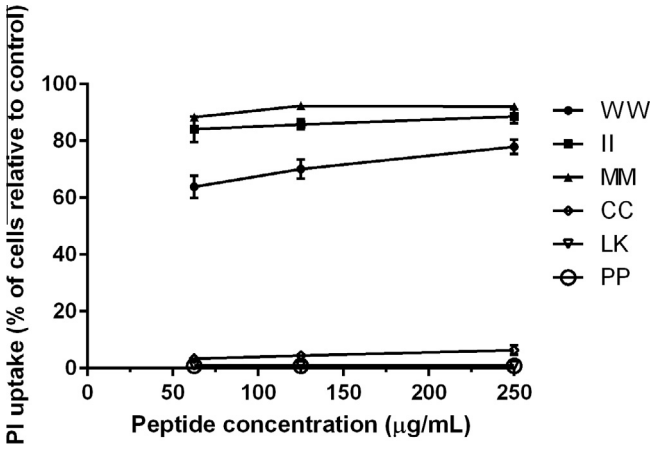

Fig. 2. Flow cytometric analysis of the mycobacterial cell membrane-permeabilizing properties of synthetic α-helical peptides. WW, MM and II induced significant membrane damage as shown by the greater uptake of PI in bacterial cells as compared to CC, PP and LK.

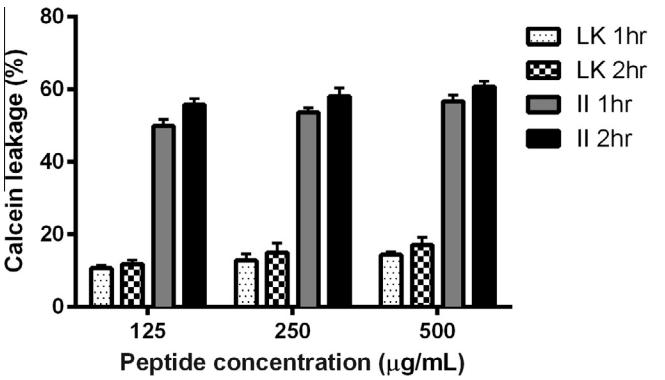

Fig. 3. Concentration- and time-dependent dye leakage from PE/PG vesicles following antimicrobial peptide treatment. II induced greater leakage as compared to LK, representative of its superior membrane-disrupting properties.

supported by previous findings that compounds inherently more injurious to membranes, as ascertained by dye leakage assays, also tend to possess enhanced antimicrobial activities [49].

Based on the MIC, FICI, and SI values, and cytotoxicity profiles of the synthetic peptide analogues, II possessed the greatest potential for practical applications and hence, was selected for further evaluation of the antimicrobial mechanisms of action against *M. smegmatis*. The surface morphology of *M. smegmatis* was visualized by scanning electron microscopy following incubation with II at 4× MIC for 2 h, and compared to controls treated with PBS. The untreated bacterial cells had regular, smooth surfaces and remained visibly intact without any extracellular debris (Fig. 4A and B). Cells treated with II however, had suffered significant structural changes. Compared to the control, cells exposed to II possessed extensively rough, corrugated surfaces covered with irregular debris (Fig. 4C and D). The significant cell surface damage induced by lethal doses of II provides evidence of the membrane-targeted mechanism of action of this peptide.

This proposed mechanism was further investigated by examining the ability of II to depolarize the cytoplasmic membrane of *M. smegmatis* using the membrane potential sensitive dye diS-C_3-5. As diS-C_3-5 partitions into the cytoplasmic membrane, its fluorescence is self-quenched due to the polarized membrane surface. Subsequent exposure to pore-forming or membrane-disrupting peptides will dissipate the membrane potential, resulting in the release of diS-C_3-5 into the medium [50]. Fluorescence recovery is then measured by spectrofluorometry and is indicative of the extent of membrane potential reduction. As seen in Fig. A4, there was a rapid, concentration-dependent surge in fluorescence intensity upon the addition of II to *M. smegmatis*. Cells exposed to II at 4× and 8× MIC produced an instantaneous increase in fluorescence signals while those treated with II at 1× MIC showed gradual dissipation of membrane potential instead.

Membrane destruction leading to loss of barrier function would result in the depletion of intracellular stores of critical components. As such, extracellular ATP levels following exposure of *M. smegmatis* to supra and sub-inhibitory concentrations of II were assessed and the findings are summarized in Fig. 5. The peptide induced concentration-dependent release of ATP from bacterial cells after 2 h, with no detectable ATP at concentrations below 15.6 μg mL^{-1}. At 4× and 8× MIC, the amount of ATP released was 106 and 132 nM respectively, an increase of approximately three to four fold as compared to ATP concentrations at MIC (33 nM).

To determine if the bactericidal activity of the peptides is associated with ATP release and membrane depolarization, killing efficiency assays were performed for II at the relevant concentrations. As shown in Fig. A5, 100% reduction in bacterial load was observed at 2×, 4× and 8× MIC while in contrast, II was only bacteriostatic at its MIC, with <1 log reduction in final CFU counts as compared to the initial inoculum. These findings suggest that the bactericidal activity of II is possibly mediated through disruption of the mycobacterial cytoplasmic membrane, with high levels of ATP release and dissipation of membrane potential, in a concentration-dependent manner.

Taken together, our results highlight that the bacterial membrane is the main target site of the synthetic cationic α-helical peptide, II. Flow cytometric analysis revealed that the formation of helical structures is crucial for rapid pore or channel formation, in agreement with previously published works [27]. Though active against mycobacteria, LK and PP did not induce significant membrane permeabilization, suggesting that they may either act via non-membrane lytic mechanisms or that the duration of drug exposure was insufficient to cause appreciable membrane damage. WW, MM and II, however, rapidly permeabilize the bacterial membrane, enabling the free diffusion of PI into the cytoplasm. Concomitantly, peptides induced immediate dissipation of the cytoplasmic membrane potential, accompanied by leakage of intracellular components as quantified by the ATP bioluminescence assay, eventually leading to cell death. Furthermore, SEM analysis revealed that the peptides possessed strong membrane-disrupting properties while calcein leakage from LUVs was

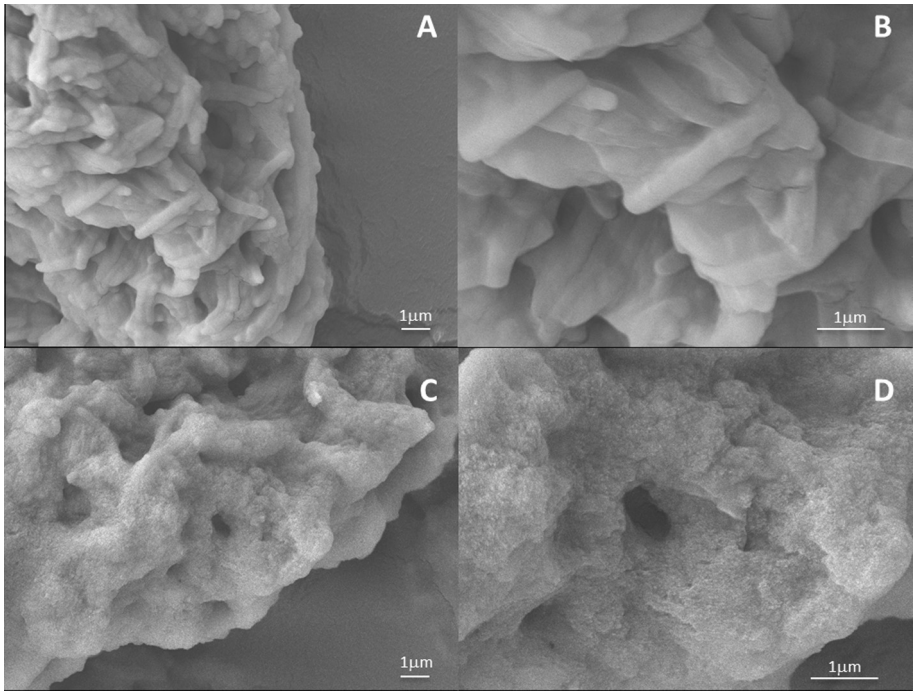

Fig. 4. SEM micrographs of *M. smegmatis* treated with II for 2 h at 4× MIC, imaged at magnifications of (C) 7500× and (D) 18,000×. Untreated cells were incubated with PBS for 2 h and similarly image at magnifications of (A) 7500× and (B) 18,000×.

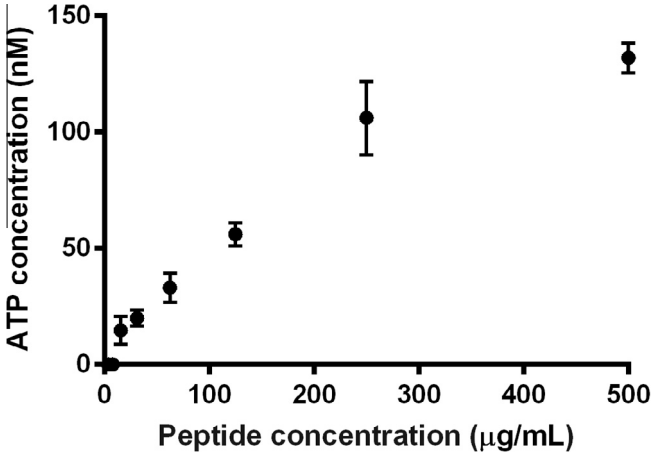

Fig. 5. Extracellular ATP release in a concentration-dependent manner after exposure of *M. smegmatis* to II for 2 h. Peptide-induced membrane damage is accompanied by leakage of intracellular content due to compromised membrane integrity.

reflective of their ability to permeabilize the lipid bilayer, resulting in the loss of intracellular contents.

4. Conclusions

In this study, six synthetic peptide analogues with varying hydrophobicity and helical propensities were assessed for their potency against *M. smegmatis*, and toxicities towards eukaryotic cells. Hydrophobic modifications produced three analogues, WW, MM and II with improved anti-mycobacterial activity. Increasing peptide hydrophobicity/helicity induced greater membrane perturbation as shown by the significant PI uptake as compared to controls during flow cytometry assays. Further, the three most hydrophobic peptides were found to interact synergistically with rifampicin, potentially mediated by enhanced intracellular access of the drug. Amongst the six, II (the isoleucine substituted peptide) was selected for elucidation of anti-mycobacterial mechanisms, given its superior selectivity index and safer toxicity profile against macrophage cells. This peptide was shown to primarily target the plasma membrane, acting rapidly in a concentration-dependent manner, and exhibiting bactericidal activity at $\geqslant 2\times$ MIC. II induced instantaneous membrane depolarization, damaged structural integrity of the membrane and caused the leakage of cellular contents within 2 h. These findings serve to deepen our understanding of the modulating effect of hydrophobicity/helicity on the anti-mycobacterial mechanisms of action and demonstrate the applicability of strategies employed here for the rational design of AMPs with the aim of improving cell selectivity and synergistic interactions when co-administered with first line antibiotics in the fight against drug-resistant tuberculosis.

Acknowledgments

The authors would like to acknowledge research funding and facilities provided by the National University of Singapore (NUS), Institute of Bioengineering and Nanotechnology (Biomedical Research Council, Agency for Science, Technology and Research, Singapore) through SERC Personal Care Programme Grant No: 1325400028. This research is supported by the Singapore Ministry of Health's National Medical Research Council under its Individual Research Grant Scheme (NMRC/1298/2011) awarded to P.R. Ee and Y.Y. Yang, President's Graduate Fellowship to J.S. Khara, NUS research scholarships to Y. Wang and X. Ke, and A*STAR AGS scholarship to Z.X. Voo.

Appendix A. Supplementary data

Supplementary data associated with this article can be found, in the online version, at http://dx.doi.org/10.1016/j.actbio.2015.09.015.

References

[1] D.A. Phoenix, S.R. Dennison, F. Harris, Antimicrobial Peptides, Wiley-VCH Verlag GmbH & Co. KGaA, Weinheim, Germany, 2013.
[2] R.E. Hancock, H.-G. Sahl, Antimicrobial and host–defense peptides as new anti-infective therapeutic strategies, Nat. Biotechnol. 24 (2006) 1551–1557.
[3] L. Yang, T.A. Harroun, T.M. Weiss, L. Ding, H.W. Huang, Barrel-stave model or toroidal model? A case study on melittin pores, Biophys. J. 81 (2001) 1475–1485.
[4] K. Matsuzaki, O. Murase, N. Fujii, K. Miyajima, An antimicrobial peptide, magainin 2, induced rapid flip–flop of phospholipids coupled with pore formation and peptide translocation, Biochemistry 35 (1996) 11361–11368.
[5] E. Gazit, I.R. Miller, P.C. Biggin, M.S. Sansom, Y. Shai, Structure and orientation of the mammalian antibacterial peptide cecropin P1 within phospholipid membranes, J. Mol. Biol. 258 (1996) 860–870.
[6] H. Sato, J.B. Feix, Peptide-membrane interactions and mechanisms of membrane destruction by amphipathic α-helical antimicrobial peptides, Biochim. Biophys. Acta 1758 (2006) 1245–1256.
[7] R. Hancock, A. Patrzykat, Clinical development of cationic antimicrobial peptides: from natural to novel antibiotics, Curr. Drug Targets Infect. Disord. 2 (2002) 79–83.
[8] S.A. Baltzer, M.H. Brown, Antimicrobial peptides – promising alternatives to conventional antibiotics, J. Mol. Microb. Biotechnol. 20 (2011) 228–235.
[9] WHO, Global Tuberculosis Report 2014, World Health Organization, Geneva, 2014.
[10] P.J. Brennan, H. Nikaido, The envelope of mycobacteria, Annu. Rev. Biochem. 64 (1995) 29–63.
[11] J. Trias, R. Benz, Permeability of the cell wall of *Mycobacterium smegmatis*, Mol. Microbiol. 14 (1994) 283–290.
[12] D.M. Yajko, C.A. Sanders, P.S. Nassos, W.K. Hadley, In vitro susceptibility of *Mycobacterium avium* complex to the new fluoroquinolone sparfloxacin (CI-978; AT-4140) and comparison with ciprofloxacin, Antimicrob. Agents Chemother. 34 (1990) 2442–2444.
[13] N. Rastogi, K.S. Goh, Action of 1-isonicotinyl-2-palmitoyl hydrazine against the *Mycobacterium avium* complex and enhancement of its activity by m-fluorophenylalanine, Antimicrob. Agents Chemother. 34 (1990) 2061–2064.
[14] A. Haemers, D. Leysen, W. Bollaert, M. Zhang, S. Pattyn, Influence of N substitution on antimycobacterial activity of ciprofloxacin, Antimicrob. Agents Chemother. 34 (1990) 496–497.
[15] D.G. Lee, H.N. Kim, Y. Park, H.K. Kim, B.H. Choi, C.-H. Choi, et al., Design of novel analogue peptides with potent antibiotic activity based on the antimicrobial peptide, HP (2–20), derived from N-terminus of *Helicobacter pylori* ribosomal protein L1, Biochim. Biophys. Acta 1598 (2002) 185–194.
[16] H. Meng, K. Kumar, Antimicrobial activity and protease stability of peptides containing fluorinated amino acids, J. Am. Chem. Soc. 129 (2007) 15615–15622.
[17] I.S. Radzishevsky, S. Rotem, F. Zaknoon, L. Gaidukov, A. Dagan, A. Mor, Effects of acyl versus aminoacyl conjugation on the properties of antimicrobial peptides, Antimicrob. Agents Chemother. 49 (2005) 2412–2420.
[18] Z. Jiang, M.P. Higgins, J. Whitehurst, K.O. Kisich, M.I. Voskuil, R.S. Hodges, Anti-tuberculosis activity of α-helical antimicrobial peptides: de novo designed L- and D-enantiomers versus L- and D-LL37, Protein Pept. Lett. 18 (2011) 241.
[19] J.S. Khara, Y. Wang, X.-Y. Ke, S. Liu, S.M. Newton, P.R. Langford, et al., Anti-mycobacterial activities of synthetic cationic α-helical peptides and their synergism with rifampicin, Biomaterials 35 (2014) 2032–2038.
[20] N. Yamamoto, A. Tamura, Designing cell-aggregating peptides without cytotoxicity, Biomacromolecules 15 (2014) 512–523.
[21] P.J. Petersen, P. Labthavikul, C.H. Jones, P.A. Bradford, In vitro antibacterial activities of tigecycline in combination with other antimicrobial agents determined by chequerboard and time-kill kinetic analysis, J. Antimicrob. Chemother. 57 (2006) 573–576.
[22] K. Rand, H. Houck, P. Brown, D. Bennett, Reproducibility of the microdilution checkerboard method for antibiotic synergy, Antimicrob. Agents Chemother. 37 (1993) 613–615.
[23] G.M. Eliopoulos, R.C. Moellering, Antibiotic Combinations, 3rd ed., The Williams & Wilkins Co., Baltimore, MD, 1991.
[24] D.S. Jacobs, W.R. DeMott, D.K. Oxley, Jacobs & DeMott Laboratory Test Handbook with Key Word Index, 5th ed., Lexi Comp, Hudson, OH, 2001.
[25] S.E. Koshlukova, T.L. Lloyd, M.W. Araujo, M. Edgerton, Salivary histatin 5 induces non-lytic release of ATP from *Candida albicans* leading to cell death, J. Biol. Chem. 274 (1999) 18872–18879.
[26] K. Lienkamp, A.E. Madkour, K.-N. Kumar, K. Nüsslein, G.N. Tew, Antimicrobial polymers prepared by ring-opening metathesis polymerization: manipulating antimicrobial properties by organic counterion and charge density variation, Chemistry 15 (2009) 11715–11722.
[27] M. Dathe, T. Wieprecht, Structural features of helical antimicrobial peptides: their potential to modulate activity on model membranes and biological cells, Biochim. Biophys. Acta 1462 (1999) 71–87.

[28] C.D. Fjell, J.A. Hiss, R.E. Hancock, G. Schneider, Designing antimicrobial peptides: form follows function, Nat. Rev. Drug Discov. 11 (2011) 37–51.
[29] M.P. Dos Santos Cabrera, M. Arcisio-Miranda, S.T. Broggio Costa, K. Konno, J.R. Ruggiero, J. Procopio, et al., Study of the mechanism of action of anoplin, a helical antimicrobial decapeptide with ion channel-like activity, and the role of the amidated C-terminus, J. Pept. Sci. 14 (2008) 661–669.
[30] L.T. Nguyen, J.K. Chau, N.A. Perry, L. De Boer, S.A. Zaat, H.J. Vogel, Serum stabilities of short tryptophan- and arginine-rich antimicrobial peptide analogs, PLoS One 5 (2010) e12684.
[31] D.-H. Chin, R.W. Woody, C.A. Rohl, R.L. Baldwin, Circular dichroism spectra of short, fixed-nucleus alanine helices, Proc. Natl. Acad. Sci. U.S.A. 99 (2002) 15416–15421.
[32] N.E. Shepherd, H.N. Hoang, G. Abbenante, D.P. Fairlie, Single turn peptide alpha helices with exceptional stability in water, J. Am. Chem. Soc. 127 (2005) 2974–2983.
[33] P. Luo, R.L. Baldwin, Mechanism of helix induction by trifluoroethanol: a framework for extrapolating the helix-forming properties of peptides from trifluoroethanol/water mixtures back to water, Biochemistry 36 (1997) 8413–8421.
[34] Y. Chen, M.T. Guarnieri, A.I. Vasil, M.L. Vasil, C.T. Mant, R.S. Hodges, Role of peptide hydrophobicity in the mechanism of action of α-helical antimicrobial peptides, Antimicrob. Agents Chemother. 51 (2007) 1398–1406.
[35] Z. Jiang, B.J. Kullberg, H. Van Der Lee, A.I. Vasil, J.D. Hale, C.T. Mant, et al., Effects of hydrophobicity on the antifungal activity of α-helical antimicrobial peptides, Chem. Biol. Drug Des. 72 (2008) 483–495.
[36] S.S. Zimmerman, H.A. Scheraga, Influence of local interactions on protein structure. I. Conformational energy studies of N-acetyl-N′-methylamides of Pro-X and X-Pro dipeptides, Biopolymers 16 (1977) 811–843.
[37] L. Piela, G. Némethy, H.A. Scheraga, Proline-induced constraints in α-helices, Biopolymers 26 (1987) 1587–1600.
[38] S. Kumar, M. Bansal, Dissecting α-helices: position-specific analysis of α-helices in globular proteins, Proteins 31 (1998) 460–476.
[39] M.K. Kim, Y.K. Kang, Positional preference of proline in α-helices, Protein Sci. 8 (1999) 1492–1499.
[40] Y. Chen, C.T. Mant, S.W. Farmer, R.E. Hancock, M.L. Vasil, R.S. Hodges, Rational design of α-helical antimicrobial peptides with enhanced activities and specificity/therapeutic index, J. Biol. Chem. 280 (2005) 12316–12329.
[41] A. Giangaspero, L. Sandri, A. Tossi, Amphipathic α helical antimicrobial peptides, Eur. J. Biochem. 268 (2001) 5589–5600.
[42] L.S. Vermeer, Y. Lan, V. Abbate, E. Ruh, T.T. Bui, L.J. Wilkinson, et al., Conformational flexibility determines selectivity and antibacterial, antiplasmodial, and anticancer potency of cationic α-helical peptides, J. Biol. Chem. 287 (2012) 34120–34133.
[43] M. Dathe, M. Schümann, T. Wieprecht, A. Winkler, M. Beyermann, E. Krause, et al., Peptide helicity and membrane surface charge modulate the balance of electrostatic and hydrophobic interactions with lipid bilayers and biological membranes, Biochemistry 35 (1996) 12612–12622.
[44] T. Tachi, R.F. Epand, R.M. Epand, K. Matsuzaki, Position-dependent hydrophobicity of the antimicrobial magainin peptide affects the mode of peptide–lipid interactions and selective toxicity, Biochemistry 41 (2002) 10723–10731.
[45] T. Wieprecht, M. Dathe, M. Beyermann, E. Krause, W.L. Maloy, D.L. MacDonald, et al., Peptide hydrophobicity controls the activity and selectivity of magainin 2 amide in interaction with membranes, Biochemistry 36 (1997) 6124–6132.
[46] B. Jacob, I.-S. Park, J.-K. Bang, S.Y. Shin, Short KR-12 analogs designed from human cathelicidin LL-37 possessing both antimicrobial and antiendotoxic activities without mammalian cell toxicity, J. Pept. Sci. 19 (2013) 700–707.
[47] M.L. Mangoni, A.C. Rinaldi, A. Di Giulio, G. Mignogna, A. Bozzi, D. Barra, et al., Structure–function relationships of temporins, small antimicrobial peptides from amphibian skin, Eur. J. Biochem. 267 (2000) 1447–1454.
[48] O. Cirioni, C. Silvestri, R. Ghiselli, F. Orlando, A. Riva, F. Mocchegiani, et al., Protective effects of the combination of α-helical antimicrobial peptides and rifampicin in three rat models of *Pseudomonas aeruginosa* infection, J. Antimicrob. Chemother. 62 (2008) 1332–1338.
[49] G.J. Gabriel, A.E. Madkour, J.M. Dabkowski, C.F. Nelson, K. Nüsslein, G.N. Tew, Synthetic mimic of antimicrobial peptide with nonmembrane-disrupting antibacterial properties, Biomacromolecules 9 (2008) 2980–2983.
[50] M. Wu, R.E. Hancock, Interaction of the cyclic antimicrobial cationic peptide bactenecin with the outer and cytoplasmic membrane, J. Biol. Chem. 274 (1999) 29–35.